Journal of Applied Mechanics Vol.10, pp.187-192 (August 2007) JSCE

# On the coupled FE - SBFE method for fracture mechanics applications

Santosh Shrestha * and Mitao Ohga **

* Dr. of Eng. Candidate, Dept. of Civil & Envn. Eng., Ehime University, Bunkyo-Cho 3, Matsuyama 790-8577
** Dr. of Eng., Professor, Dept. of Civil & Envn. Eng., Ehime University, Bunkyo-Cho 3, Matsuyama 790-8577

A coupling of the traditional finite element method (FEM) with the recently developed scaled boundary finite element method (SBFEM) is applied for analyzing two-dimensional (2D) linear elastic fracture mechanics problems. Since shape functions of SBFEM are compatible with finite element shape functions and no discontinuity occurs across the interface, the FEM can be coupled with SBFEM without any special treatment that require for the coupling with others methods. The SBFEM has an ability to analytically compute stress and displacement field of singularities region at the crack-tip more accurately without any *a priori* assumptions. The SBFEM was employed for the modelling of near cracks region, where their capabilities can be exploited to the greatest benefit, and the FEM for areas away from cracks, where no singularities in the stress fields are expected to arise. The effectiveness of the proposed coupled method was examined by computing the mixed mode SIFs and T-stress in 2D cracked structures. The computed results are in excellent agreement with those obtained from existing numerical methods.

*Keywords: finite element method, scaled boundary finite element method, coupling, fracture parameters, SIFs, T-stress*

## 1. Introduction

The modelling of fracture and damage is one of the dominant research areas in solid mechanics today in order to implement simulations essential for failure prediction of engineering structures[1]. For these modelling, the finite element method (FEM) is obviously a dominant computational method in engineering because of its great flexibilities and wide range of applicability. Unfortunately, the FEM has some limitations and is inefficient to deal with fracture mechanics problems. In order to capture the stress singularities occurring near crack-tip/ discontinuity (material or geometric), it is necessary a precise discretization of the crack-tip region / discontinuity, which reduces its efficiency, or the use of specialized elements of the singular type. When studying crack growth phenomena, working with the FEM can become cumbersome, because the precise representation and discretization of the discontinuity must be preformed for each configuration of the discontinuity during crack growth. In order to overcome these deficiencies, considerable research has been directed towards developments of sophisticated mesh generation procedures or adaptive techniques such as hybrid crack element (HCE) method[2], extended finite element method (XFEM)[3], and S-version FEM (s-FEM)[4]. On the other hand, compared to the FEM, the boundary element method (BEM) is particularly attractive for the analysis of linear elastic fracture mechanics (LEFM) problems. However, it needs complicated mathematics procedures with fundamental solution and the standard boundary element formulation is not effective for numerical modeling of certain crack problems such as, cracks as narrow slits with upper and lower surfaces slightly separated[5]. More recently, the dual boundary finite method[6], displacement discontinuity BEM (DDBEM)[5] and Green's function BEM[7], which are in developing stage, seems to be an efficient way of modeling crack problems in BEM. Likewise, the meshless methods[8,9] have been developed and used with increasing frequency over the last decade. The meshless methods are very flexible concerning geometrical updating of the model but it does not delete the necessity of the modal rearrangement to keep the accuracy of the calculation during crack propagation. As compared with the standard FEM approach, the meshless methods generally require more computational time to solve the system equations[10,11]. Even though much achievement has been made in crack modeling techniques, it is necessary to have excellent solutions surrounding the tips, including the asymptotic behaviour, where the fracture process occurs[12].

Recently, the scaled boundary finite element method (SBFEM)[13] developed by Wolf and Song is emerging as an efficient alternative approach in order to overcome the above mentioned deficiencies of the FEM. Authors[14-15] and other researchers[16-19] have presented the versatility of SBFEM to compute the fracture parameters - stress intensity factors (SIFs), *T*-stress and higher order terms of the crack tip stress field. The

SBFEM has a significant advantage over the FEM and the BEM to analytically compute stress and displacement field of singularities region at the crack-tip without any *a priori* assumptions so that accurate fracture parameters can be calculated directly from the definition. Likewise, the SBFEM has its unique properties that no discretizations of side-face boundaries are required [13], so that the computation cost can be further reduced. Because of these specific advantages of SBFEM, fine mesh or special singular element that required near crack-tip in FEM can be avoided. Moreover, for crack propagation simulation, authors[20, 21] have recently demonstrated the SBFEM's flexibility than FEM and proposed a simple remeshing procedure than BEM.

However, the SBFEM has certain limitations. It requires the scaling of material variations with relative to the so-called scaling center and many sub-divisions to deal complex geometry problem that leads to increase the computational load. Besides, it is considered linear elastic material behaviors for elastostatics problems within the domain. These SBFEM's weaknesses can be FEM's strengths. Therefore, it is often desirable to couple the SBFEM with FEM. To our knowledge, none of the previous studies have addressed the fracture analysis by a coupled FE-SBFEM.

The main aim of this paper is to couple the FEM with SBFEM to fracture mechanics applications. It is often advantageous to use SBFEM only in the sub-domains closed to cracks, where their capabilities can be exploited to the greatest benefit and the conventional FEM in areas away from cracks, where no singularities in the stress fields are expected to arise. Since shape functions of SBFEM are compatible with finite element shape functions and no discontinuity occurs across the interface, coupling of FEM with SBFEM is a straightforward process and easy than that with others methods such as Meshless and BEM. Numerical examples are considered to compute SIFs and T-stress of 2D cracked structures. The computed results are in excellent agreement with those obtained from existing numerical methods

## 2. Review of scaled boundary finite element method

The scaled boundary finite element method is a new semi-analytical fundamental solution-less BEM based on FEM[13]. It is BEM-like method that decreases the spatial dimension by one. However, it does not require a fundamental solution. It is based on the FEM formulation. The solution is analytical in the radial direction and more accurate than the circumferential direction. It is, therefore, semi-analytical method that it transforms the partial differential equation of a variety of linear problems into ordinary differential equations. These ordinary differential equations can be solved analytically in radial direction and the coefficients of these equations are determined by the finite element approximation in the circumferential direction.

The SBFEM formulation based on weighted residual method and virtual work principle has been presented in Ref [13, 22], respectively and authors have summarized the derivation in Ref.[14] for bounded domain. The summary is reproduced here with some modifications for convenience as follows.

The basic concept of the SBFEM is presented in Fig. 1. The figure shows that the discretized boundaries are scaled with

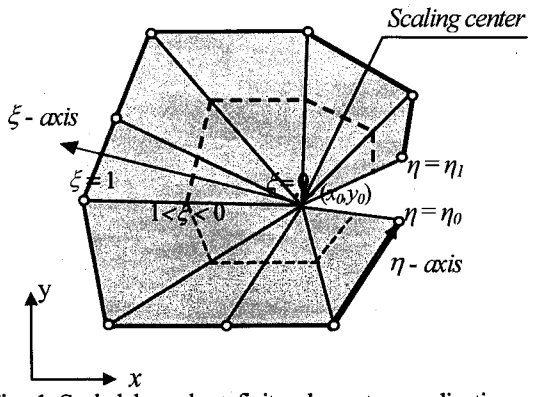

Fig. 1 Scaled boundary finite element co-ordination system in bounded domain with side faces.

respect to the so-called 'scaling center' by introducing a scaled boundary coordinate system with a radial coordinate, $\xi$, and a circumference coordinate, $\eta$. The displacements at any point in the domain defined by scaled boundary coordinates ($\xi$, $\eta$) can be expressed in the form

$$\{u(\xi,\eta)\} = \sum_{i=1}^{n} N_i(\eta)\{u_i(\xi)\} = [N(\eta)]\{u(\xi)\} \qquad (1)$$

where $N(\eta)$ is the shape function in the circumferential direction, which are constructed as in FEM. $u(\xi)$ defines the displacements along the radial lines. The key relations defining in SBFEM for plane problems are as follows. (See Ref. [14] for details)

According to these derivations, the governing equations of the SBFEM for elastostatics is as follows

$$[E^0]\xi^2\{u(\xi)\}_{,\xi\xi} + [[E^0]+[E^1]^T-[E^1]]\{u(\xi)\}_{,\xi} - [E^2]\{u(\xi)\} = 0 \qquad (2)$$

$$\{P\} = [E^0]\{u(\xi)\}_{,\xi} + [E^1]^T\{u(\xi)\} \qquad (3)$$

where $\{u(\xi)\}$ and $\{P\}$ are the nodal displacements and nodal forces respectively, and the $[E^0]$, $[E^1]$, $[E^2]$ are the coefficient matrices which depend on the material properties and the geometry of domain/sub-domain boundaries. These matrices can be computed element by element over the boundary, and assembled together for the entire boundary in the same manner as the stiffness matrix is determined for the entire domain in the standard finite element method.

The general solution of Eq. (2) is in the form

$$\{u_h(\xi)\} = \sum_{i=1}^{n} c_i \xi^{-\lambda_i}\{\phi_i\} \qquad (4)$$

where the exponents $\lambda$ and vectors $\phi$ are represented as a radial scaling factor and a displacement modes shapes. The integration constants, $c$ represent the contribution of each mode to the solution, and are dependent on the boundary conditions.

Substituting this solution into Eq. (2) yields the quadratic eigenproblem

$$\begin{bmatrix} [E^0]^{-1}[E^1]^T & -[E^0]^{-1} \\ [E^1][E^0]^{-1}[E^1]^T - [E^2] & -[E^1][E^0]^{-1} \end{bmatrix} \begin{Bmatrix} \phi \\ p \end{Bmatrix} = \lambda \begin{Bmatrix} \phi \\ p \end{Bmatrix} \qquad (5)$$

The solution of this eigenproblem yields $2n$ displacement modes, where $n$ is the total degrees of freedom (DOFs) on the boundary discretization, and hence is also the size of the coefficient matrices. The eigenvectors contain the modal displacements and the equivalent modal node forces. For a

bounded domain $0 \le \xi \le 1$only the $n$ modes with non-negative real components of $\lambda$ lead to finite displacements at scaling center. This subset of $n$ nodes is denoted by $\Phi = \{\varphi_1 \varphi_2 \varphi_3 \ldots \varphi_n\}$ and corresponding equivalent model forces

From Eqs. (3) and (4), the nodal forces becomes

$$\{P\} = ([E^0]\lambda + [E^1]^T)\Phi c \tag{6}$$

On the boundary or interface of sub-domain, Eq. (4) becomes

$$\{u_n\} = \Phi c \tag{7}$$

where $u_n$ is the nodal displacements on the discretized boundary the integration constant, $c = \{c_1 c_2 c_3 \ldots c_n\}$.

After substituting $c$ from the Eq. (7), the Eq. (6) becomes

$$\{P\} = ([E^0]\Phi\lambda\Phi^{-1} + [E^1]^T)\{u_n\} \tag{8}$$

Therefore, the equilibrium equation is as follows

$$\{P\} = [K^s]\{u_n\} \tag{9}$$

and stiffness matrix of the sub-domain/ domain

$$[K^s] = [E^0]\Phi\lambda\Phi^{-1} + [E^1]^T \tag{10}$$

The displacement fields and stress fields inside the sub-domain/ domain can be obtained using

$$\{u(\xi,\eta)\} = [N(\eta)]\sum_{i=1}^{n} c_i \xi^{-\lambda_i}\{\phi_i\} \tag{11}$$

$$\{\sigma(\xi,\eta)\} = [D]\sum_{i=1}^{n}[c_i \xi^{-\lambda_i - 1}[-\lambda_i[B^1(\eta)] + [B^2(\eta)]]\{\phi_i\}] \tag{12}$$

where D is the elasticity matrix and $B^1(\eta)$ and $B^2(\eta)$ are relevant matrices depending on geometry of the sub-domain / domain boundary only.

## 3. SBFEM for fracture analysis

To compute the fracture parameters i.e. SIFs and $T$-stress and higher order terms of the crack-tip stress fields, authors have presented two different formulations by comparing the classical linear elastic field solution (Williams' eigenfunction series) in the vicinity of a crack-tip with the scaled boundary finite element stress and displacement field solution at any point ahead of crack-tip in Refs.[14) and 15)] respectively. In these formulations, the so-called 'scaling center' of SBFEM is considered at the crack-tip, as shown in Fig. 2 and the stress/displacement field along the radial direction emanating from the crack-tip where the stress singularity occurs are analytically calculated to approximate the crack-tip along the line of propagation of the crack. According to Ref. [14)], the mixed mode SIFs and T-stress of the stress fields are computed by the following relations.

$$K_I = c\hat{\sigma}_{yy}\sqrt{2\pi\hat{r}} \tag{13}$$

$$K_{II} = c(\hat{\sigma}_{xy})\sqrt{2\pi\hat{r}} \tag{14}$$

$$T = c(\hat{\sigma}_{xx}) \tag{15}$$

where $K_I$ ,$K_{II}$ and $T$ are SIFs for mode I and mode II and T-stress, respectively and $\hat{\sigma}_{xx}$ , $\hat{\sigma}_{yy}$ and $\hat{\sigma}_{xy}$ are the stress components along the axis as shown in Fig. 2. $\hat{r}$ is the radial distances of the boundary nodes from scaling center, and $c$ is the integration constant. Only the basic equations of the proposed formulation are presented here. For a more detailed description see Ref.[14)].

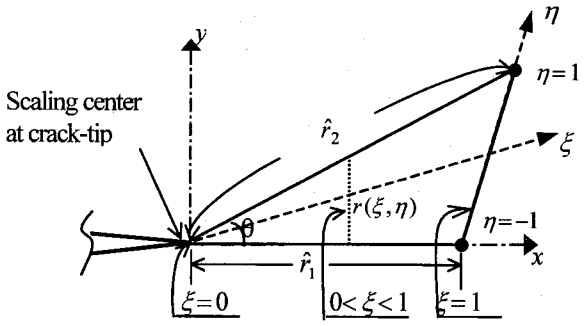


Fig. 2. SBFEM element with different coordinates

## 4. Discrete equations of FEM and SBFEM

Consider a two-dimensional elastostatics problem of solid mechanics in domain $\Omega$ bounded by $\Gamma$. The equilibrium equations is the following differential equation

$$\nabla \cdot \sigma + b = 0 \quad \text{in} \quad \Omega \tag{16}$$

This equation must be satisfied at every point within the domain, $\Omega$. Here $\sigma = \Delta\varepsilon$ is the stress vector, which corresponds to the displacement field $u = \{u, v\}^T$, b is the body force vector, and $\nabla$ is the divergence operator.

The boundary conditions on displacements and surface tractions are given as follows:

$$u = \bar{u} \quad \text{on} \quad \Gamma_u \tag{17a}$$

$$\sigma \cdot n = \bar{t} \quad \text{on} \quad \Gamma_t \tag{17b}$$

where, ū and t are the vectors of prescribed displacements and surface tractions at the boundary and the superposed bar denotes prescribed boundary values, **n** is a unit normal outward to domain $\Omega$. $\Gamma_t$ and $\Gamma_u$ are the positions of the boundary where tractions and displacements are prescribed, respectively.

The alternative form of the Eqs. (16) and (17 ) is the virtual work statement as follows

$$\int_\Omega \delta\varepsilon^T \sigma d\Omega - \int_\Omega \delta u^T p d\Omega - \int_\Gamma \delta u^T \bar{t}.d\Gamma = 0 \tag{18}$$

The FEM and SBFEM use the variation given in the equation. Using the virtual work, FEM reduce the non-homogenous set of governing partial differential equations (PDEs) to a set of linear equations, but, as mentioned above, SBFEM reduces the PDEs to a set of ordinary differential equations, which can be solved analytically. The resulting equations represent a stronger equilibrium requirement than the linear finite element equations.

The approximation of the displacements $\{u(x,y)\}$ at any point in the FEM can be written as [23)]

$$\{u(x,y)\} = \sum_{i=1}^{n} \Psi_i(x,y)u_i = [\Psi(x,y)]\{\hat{u}\} \tag{19}$$

where $\Psi(x, y)$ is the FEM shape functions and $\hat{u}$ is the nodal displacement. From Eqs. (18) and (19), the equilibrium equation resulting from FEM formulation can be written as

$$[K^f]\{\hat{u}\} = \{P\} \tag{20}$$

where $[K^f]$ is the stiffness matrix, and $P$ is the force vectors for FEM and superscript, $f$ designate for the FEM.

For the SBFEM, the approximation of displacement (Eq. (1)) and the equilibrium equations (Eq. (9)) have been given in Section 2.

## 5. Coupling the FE - SBFE methods

Consider a 2D problem domain $\Omega$ is divided into two non-overlapping domains – $\Omega_{SBFEM}$, SBFEM domain and $\Omega_{FEM}$, FEM domain, i.e. $\Omega = \Omega_{SBFEM} \cup \Omega_{FEM}$, with interface boundary, $\Gamma_i$ as shown in Fig. 3. In Fig. 3, $e$ (white circle), $s$ (gray circle), and $i$ (black circle) present the nodes on FEM region, SBFEM region and interface boundary respectively. The interface boundary possesses displacement compatibility and force equilibrium in coupling $\Omega_{SBFEM}$ and $\Omega_{FEM}$. This means that

$$u_{i(SBFEM)} = u_{i(FEM)} \tag{21a}$$

$$P_{i(SBFEM)} + P_{i(FEM)} = 0 \tag{21b}$$

where $u_{i\ (SBFEM)}$, $u_{i\ (FEM)}$, $P_{i\ (SBFEM)}$, and $P_{i\ (FEM)}$ are the displacements and forces on the interface boundary obtained by SBFEM and FEM respectively.

Since the SBFEM shape function is compatible with FEM shape function, the displacement compatibility equation (21a) along the interface can be written as

$$\{u_i(x,y)\} = [\Psi(x,y)]\{\hat{u}\} = [N(\eta)]\{u\} \quad \text{over} \quad \Gamma_i \tag{22}$$

These compatibility equations can be satisfied exactly over the entire interface as the SBFEM region has some number of degrees of freedom controlling the approximation.

The equilibrium equations, i.e. Eqs. (20) and (9) can be written in matrix form as follows

$$\begin{bmatrix} K^f_{ee} & K^f_{ei} \\ K^f_{ie} & K^f_{ii} \end{bmatrix} \begin{Bmatrix} u_e \\ u_i \end{Bmatrix} = \begin{Bmatrix} P_e \\ P_i \end{Bmatrix} \tag{23}$$

$$\begin{bmatrix} K^s_{ss} & K^s_{si} \\ K^s_{is} & K^s_{ii} \end{bmatrix} \begin{Bmatrix} u_s \\ u_i \end{Bmatrix} = \begin{Bmatrix} P_s \\ P_i \end{Bmatrix} \tag{24}$$

where, the subscripts, $i$, $e$ and $s$ designate interaction nodes, and non-interaction nodes for the FEM and SBFEM region as shown in Fig.3, respectively and superscript, $s$ designate for the SBFEM.

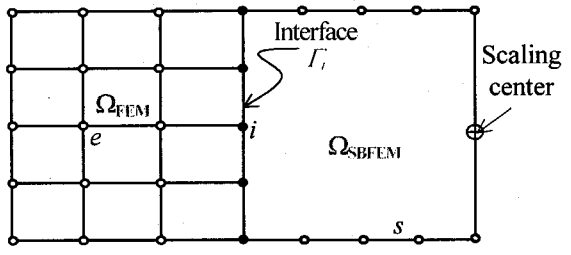


Fig. 3 Domains contains SBFEM and FEM regions

Due to the compatibility of the displacements and equilibrium of the forces at the interaction nodes between FEM and SBFEM regions, the stiffness matrices of FEM can be added to the stiffness matrix of SBFEM as follows

$$\begin{bmatrix} K^f_{ee} & K^f_{ei} & 0 \\ K^f_{ie} & K^f_{ii} + K^s_{ii} & K^s_{is} \\ 0 & K^s_{si} & K^s_{ss} \end{bmatrix} \begin{Bmatrix} u_e \\ u_i \\ u_s \end{Bmatrix} = \begin{Bmatrix} P_e \\ 0 \\ P_s \end{Bmatrix} \tag{25}$$

Eq. (25) is full system equation of the coupling method. The stiffness matrices of both the methods can be assembled to form the system stiffness matrix as usually used in the FEM.

## 6. Numerical examples

A computer coding of the coupled FE-SFEM in MATLAB was developed on the base of above coupling formulation. Then, the effectiveness of the coupled method was demonstrated to perform linear-elastic fracture analysis, especially the analysis of stress field near crack-tip of crack specimens. The following two fracture specimens were simulated.

i) A three-point bending beam, and
ii) A single edged cracked plate

The first was considered as a single loading (Mode I) condition problem while second was considered for mixed mode (Mode I & II) problem. The main objective of the analysis is to compute the fracture parameters – SIFs and T-stress. As mentioned above, the SBFEM has the greatest benefit in the discretization near crack region and it can deal more accurately and efficiently the stresses near the crack than FEM. Therefore, near crack region was modelled from SBFEM and other regions are modelled from FEM. The discretization employed in this study consisted of three-node iso-parametric quadratic line elements on the boundary for SBFEM region and eight-node iso-parametric quadratic plane elements for FEM regions. For the fracture parameters computation, only the stress along the radial line passing through first node of first element of SBFEM, as shown in Fig. 2, was calculated to approach the crack-tip along its line of propagation. The scaling center was placed at the crack-tip in SBFEM mesh and, therefore, the straight crack face and the face ahead of the crack-tip were not discretized.

### 6.1 A three-point bending beam

The first problem is a three-point bending beam with single edge crack at the middle. The schematic diagram is as shown in Fig. 4, where $L$ and $D$ are the span and depth of beam

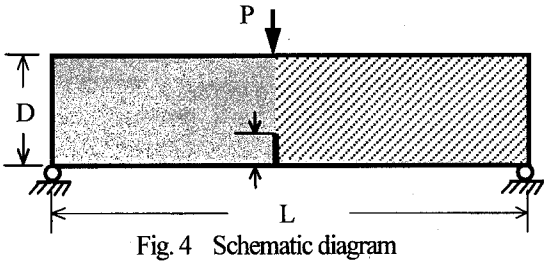


Fig. 4 Schematic diagram

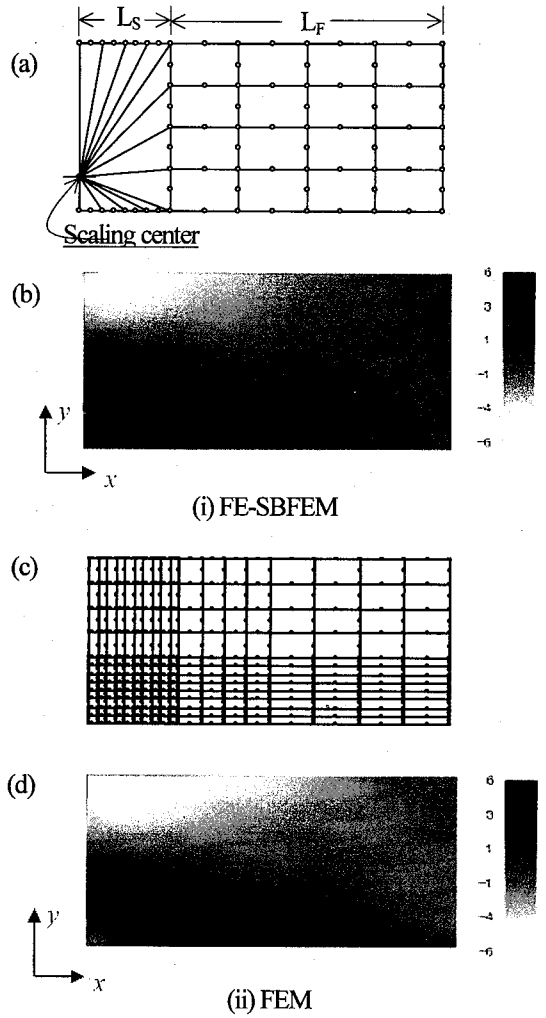


Fig. 5 Analytical Models and Stress, $\sigma_x$ contour of (*i*) FE- SBFEM and (ii) FEM

respectively and $a$ is the crack length. The applied point load per unit thickness was P = 1 unit at middle as shown in Fig 4. The analyses were carried out using plane strain condition with Young's modulus $E$ = 1.0 and Poisson's ratio $\nu$ = 0.3. Unit thickness was assumed for the analysis. All units are consistent with that of $E$. Only a half of the specimen (hatched portion in schematic diagrams) was modeled by virtue of symmetry.

The problem was analysed to compute the SIF and T-stress with span to depth ratio $L/D$ = 4 and the relative crack length, $a/D$ = 0.2. A typical FE-SBFEM model with 166 DOFs and $L_S/L_F$ = 0.25 used for analysis is given in Fig. 5 (a), where $L_S$ and $L_F$ are length of SBFEM region and FEM region respectively. To demonstrate the efficiency of the coupled method, the problem was also analysed using FEM and compared the stress along the perpendicular direction of crack face, $\sigma_x$. The FEM model with 1418 DOFs is shown in Fig .5 (c). Fig. 5 (b) and 5 (d) are presented the stress contours of the FE-SBFM coupled method and FEM method results respectively. It shows that the coupled method's result with less than 15 percentage DOFs of FEM is significantly similar result with the FEM result.

Then, the fracture parameters – SIFs and T-stress were computed using Eqs. (13) and (15) for different domain size of the SBFEM and FEM. The computed results of the normalized SIFs, $K_I/\sigma_0(\pi a)^{1/2}$ and the normalized T-stress, $T/\sigma_0$, for three different length ratios, $L_S/L_F$ are presented in the Table 1, where,

Table 1 Computed results

| $L_S/L_F$ | Normalized SIFs | | Normalized T-stress | |
|---|---|---|---|---|
| | Present | Ratio | Present | Ratio |
| 0.25 | 0.3101 | 0.99 | 0.2353 | 1.00 |
| 0.50 | 0.3090 | 0.99 | 0.2361 | 1.00 |
| 0.75 | 0.3083 | 0.99 | 0.2367 | 1.01 |

* Ratio with the values (0.312 & 0.2355) from [22]

$\sigma_0 = 3PL/2D^2$ and the 'ratio' is the comparison of the computed results with respect to the references results. These FE-SBFEM results of the normalized SIFs are compared with the results obtained by Guinea et al. (1998), while the computed normalized $T$–stress are compared with the results obtained by HCE method from Ref.[24]. The comparison shows that FE-SBFEM results are in an excellent agreement with the references values and significantly similar results in all the domain size, i.e. no major effects in the results due to domain size.

### 6.2 A single edged cracked plate

A single edged cracked plate with fixed at the one end and subjected shear stress of $\tau$ = 1 unit on the other end was simulated for mixed mode fracture parameters computation. It is a widely used benchmark example for mixed mode crack problems. The schematic diagram is shown in Fig. 6 (a), and the parameters are: $a$ = 3.5, $W$ = 7 and $L$ = 16. Young's modulus $E = 10^5$ and Poisson's ratio $\nu$ = 0.25. All units are consistent with that of $E$.

For the analysis, whole structure was modeled with single SBFEM domain near crack-tip and two FEM domains for far field. The FE-SBFEM analytical model is shown in Fig. 6 (b) where ' + ' sign presents so-called the scaling center of the SBFEM. The scaling center was placed at crack-tip to compute the stress along the radial line ahead of crack-tip as a necessary condition of SBFEM's fracture mechanics formulation presented by authors. The computed mixed mode SIFs and T-stress values obtained from Eqs. (13) to (15) were compared with those of HCE method from Refs. [2], respectively in Table 2. It shows that the computed SIFs and T-stress are in good agreement with

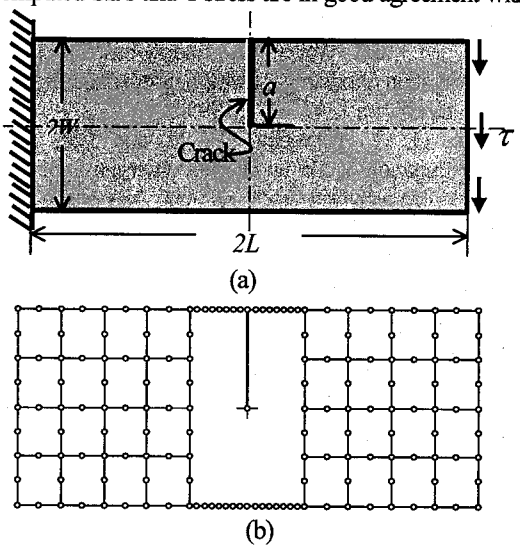


Fig. 6 (a) Schematic diagram and (b) Analytical model of FE- SBFEM

the literature results with less than 2% deviation.

Table 2 Comparison of fracture parameters

| Fracture Parameters | Present FE-SBFEM | HCE [2] | Error % |
|---|---|---|---|
| $K_I$ | 33.89 | 34.00 | 0.32 |
| $K_{II}$ | 4.561 | 4.550 | 0.24 |
| T-stress | 2.7259 | 2.6864 | 1.47 |

## 7. Conclusion

In this paper, a coupling of the newly developed scaled boundary finite element method and the traditional finite element method has been implemented for two-dimensional linear-elastic analysis of fracture mechanics problems. Since shape functions of SBFEM are compatible with finite element shape functions and no discontinuity occurs across the interface, the coupling of FEM with SBFEM is a straightforward process and the coding of SBFEM can be easily inserted in FEM coding. The SBFEM was used to model near crack region, where their capabilities can be exploited to the greatest benefit, and FEM in areas away from cracks. When compared with FEM, the complexity of crack modeling can be significantly reduced by the coupled method. The numerical examples show that the efficiency and accuracy of the proposed coupled method for analyzing two-dimensional linear elastic fracture mechanics problems.

Indeed, the coupled method has been applied here for only simple two-dimensional bounded problems with single crack for the computation of fracture parameters – SIFs and T-stress under single (Mode I) and mixed mode conditions. It can be easily applied into complex geometry, multi-cracks, three-dimensional and unbounded problems by extending the present approach. Moreover, the formulation has been so far limited to a linear elastic fracture parameters computation; it can be extended to crack propagation simulation and non-linear fracture analyses, which will be appeared in the authors' forthcoming publication.

## References


1) Xie, M., and Walter H., Energy-based cohesive crack propagation modeling, *Journal of Engineering Mechanics, ASCE*, 121, pp 1349-1358, 1995.
2) Xias, Q. Z., Karihaloo, B. L. and Liu, X.Y., Direct determination of SIF and higher order terms of mixed mode cracks by a hybrid crack element. *International Journal of Fracture*, 125, pp 207-225, 2004.
3) Liu, X.Y., Xias, and Q. Z., Karihaloo, B.L., XFEM for direct evaluation of mixed mode SIFs in homogeneous and bi-materials. *Int. J. Num. Meth. Engg*, 59, pp 1103-1118, 2004.
4) Okada, H., Endoh, S. and Kikuchi, M., On fracture analysis using an element overlay technique, *Engineering Fracture Mechanics*, 68, pp 1609-1630, 2005.
5) Yan, X., An efficient and accurate numerical method of stress intensity factors calculation of a branched crack, *ASME Journal of Applied Mechanics*, 72, pp 330-340, 2005.
6) Portela, A., and Aliabadi, M. H., The dual boundary element method: effective implementation for crack problems, *Int. J. Num. Meth. Engg*, 33, pp. 1269–1287, 1992.
7) Silveira, N.P.P., Guimaraes, S. & Telles, J.C.F. A numerical Green's function BEM formulation for crack growth simulation, *Engineering Analysis with Boundary Elements*, 29, pp. 978–985, 2005.
8) Rao B. N. and Rahman S., An efficient meshless method for fracture analysis of cracks, *Computational Mechanics*, 26, pp. 398-408, 2000.
9) Nagashima, T., Omoto, Y. and Tani, S., Stress intensity factor analysis of interface cracks using X-FEM, *Int. J. Num. Meth. Engg*, 56, pp 1151-1173, 2003.
10) Rao B. N. and Rahman S., A coupled meshless-finite element method for fracture analysis of cracks, *Int. J. of Pressure Vessels and Piping*, 78, 9, pp. 647-657, 2001.
11) Liu G.R. and Gu Y.T., *An introduction to meshfree methods and their programming*. Springer Press, Berlin, 2005.
12) Meyer, A., Rabold, F. and Scherzer, M., Efficient finite element simulation of crack propagation using adaptive iterative solvers, *Communications in Numerical Method in Engineering*, 22(2), pp. 93-108, 2006.
13) Wolf J.P., *The Scaled Boundary Finite Element Method*: John Wiley & Sons Ltd, 2003.
14) Shrestha, S. and Ohga, M, An efficient method for computation of singular and higher order terms of a crack-tip stress field, *Journal of Applied Mechanics* JSCE, 8, pp. 171-178, 2005.
15) Shrestha, S. and Ohga, M., An efficient computational method for stress concentration problems, *Structural Engineering and Mechanics*, 22, pp. 613-630, 2006.
16) Song, C., Wolf J. P., Semi-analytical representation of stress singularity as occurring in cracks in anisotropic multi-materials with the scaled boundary finite-element method. *Computers and Structures*, 80, pp 183-197, 2002.
17) Song C., A super-element for crack analysis in the time domain. *Int. J. Num. Meth. Engg*, 61, pp 1332-57, 2004.
18) Song, C., Evaluation of power-logarithmic singularities, *T*-stresses and higher order terms of in-plane singular stress fields at cracks and multi-material corners, *Engineering Fracture Mechanics*, 72, pp. 1498-1530, 2005.
19) Chidgzey, S.R. and Deeks, A.J., Determination of coefficients of crack-tip asymptotic fields using scaled boundary finite element method, *Engineering Fracture Mechanics*, 72, pp. 2019-2036, 2005.
20) Shrestha, S., Ohga, M and Taniwaki, K., Computation of SIFs of the branched crack by scaled boundary finite element method, *Journal of Structural Engineering*, JSCE, 52A, pp. 133-140, 2007.
21) Shrestha, S., Ohga, M and Taniwaki, K., On the crack propagation simulation using scaled boundary finite element method, *Symposium on 'The Scaled Boundary Finite Element Method' at The Tenth East Asia-Pacific Conference on Structural Engineering and Construction, Bangkok, Thailand*, pp. 413-418, 2006.
22) Deeks. A. J. and Wolf, J. P., A virtual work derivation of the scaled boundary finite element method for elastostatic, *Computational Mechanics*, 28, pp 489-509, 2002.
23) Cook, R. D., Malkus, M.S., and Plesha, M.E., *Concept and application of finite element analysis*, John Wiley & Sons Ltd, Canada, 1989.
24) Karihaloo, B. L. and Xias, Q. Z., Higher order terms of the crack tip asymptotic field for a notched three-point bend beam. *Int. J. of Fracture*, 112, pp 111-128, 2001.


**(Received April 12, 2007)**